Int. J. Electrochem. Sci., 9 **(2014)** 2696 - 2715

International Journal of
ELECTROCHEMICAL
SCIENCE
www.electrochemsci.org

Carboxylic Acids as Corrosion Inhibitors for Cu, Zn and Brasses in Simulated Urban Rain

Gregor Žerjav and Ingrid Milošev[*]

Jožef Stefan Institute, Department of Physical and Organic Chemistry, Jamova 39, SI-1000, Ljubljana, Slovenia
[*]E-mail: ingrid.milosev@ijs.si

Received: 12 December 2013 / *Accepted:* 14 January 2014 / *Published:* 2 March 2014

Carboxylic acids (hexanoic, decanoic, myristic and stearic) were studied as corrosion inhibitors for Cu, Zn, Cu10Zn and Cu40Zn in simulated urban rain, using electrochemical measurements. The surfaces of Cu, Zn and brasses were modified by immersion in ethanol solutions of carboxylic acids of various molarities (0.01 M to 0.1 M). Times of immersion were between 1 min and 6 days. The effect of surface etching was also studied. All carboxylic acids formed hydrophobic, self-assembled layers with a contact angle over 90°. Carboxylic acids with longer carbon chains were better corrosion inhibitors. The formation of self-assembled layers was a rapid process, high values of inhibition effectiveness being observed after only one minute of immersion. Myristic and, particularly, stearic acids are good inhibitors of Cu and brasses, providing protection of >95 %, even at low molarities. Both acids were less effective for Zn with up to 60 % effectiveness.

Keywords: carboxylic acid, self-assembled layers, hydrophobicity, corrosion inhibition, copper

1. INTRODUCTION

Copper is a very useful material because of its excellent electrical and thermal conductivity properties. To improve its mechanical properties, copper is alloyed with Zn to produce brasses. Copper and brasses provide superior functions in many applications, as fresh water supply lines and plumbing fittings, in architecture, heat exchangers and condensers, in industrial, chemical and power-generating plants, etc. During exposure of copper, zinc and brasses to various environments however, they are subjected to corrosion. There are many ways to protect them [1,2,3,4,5], one being to modify the metal surface to make it hydrophobic and thus not wetted by aqueous liquids. Carboxylic acids ($CH_3(CH_2)_mCOOH$) have been used to generate hydrophobic surfaces on Al [6,7,8,9,10], Cu [11,12,13,14,15,16], bronze [17], Mg [18], Zn [19,20], Ti [21], etc. They form self-assembled layers

by adsorption to the positively charged metal surfaces via their carboxyl groups, producing a hydrophobic layer [10,15,16, 22].

Surface roughness has an impact on the contact angle of a surface [7,15,23,24,25]. There are two wetting regimes, homogenous and heterogeneous, depending on how the liquid fills up the roughness grooves [26]. Wenzel, Cassie and Baxter studied the influence of surface roughness on the contact angle. For a homogeneous wetting regime, in which the liquid fills up the roughness grooves, the Wenzel equation is:

$$\cos\Theta_W = r\cos\Theta_Y , \quad (1)$$

where Θ_W is the Wenzel contact angle and Θ_Y the Young contact angle. The roughness ratio r is defined as the atio of the true area of the solid surface to its nominal area. This equation shows that, when a surface is hydrophobic, roughness increased the contact angle [26]. The Cassie-Baxter equation describes the heterogeneous wetting regime, in which air bubbles are entrapped inside the roughness grooves:

$$\cos\Theta_{CB} = r_f\cos\Theta_Y + f - 1, \quad (2)$$

where Θ_{CB} is the Cassie-Baxter contact angle, f is the fraction of the projected area of the solid surface that is wet by the liquid and r_f is the roughness ratio of the wet area. Surface roughness plays an important role in both wetting regimes.

The length of the carbon chain of the carboxylic acid affects the properties of the self-assembled layer. Boiser et al. tested four different monocarboxylic acids, differing in their carbon chain length, as a post-treatment for aluminium alloy AA2024 that had been anodised in tartaric-sulphuric acid. Stearic acid, with the longest chain, provided the most effective barrier to corrosion in 0.5 M Na_2SO_4 [10]. Decanoic, myristic and stearic acids formed hydrophobic layers with contact angles between 110° and 120˚, while hexanoic acid formed a layer with contact angle around 50˚. Carbon chain length thus influenced the hydrophobicity of the layer. Wang et al. [16] showed that the carbon chain length of carboxylic acid is critical for obtaining a stable superhydrophobic coating (contact angle above 150˚) on Cu.

In this study we investigated the use of carboxylic acids to modify the surfaces of Cu, Zn, Cu10Zn and Cu40Zn in order to increase their hydrophobicity and hence corrosion resistance. Hexanoic acid as a short chain, decanoic acid as a medium chain and myristic and stearic acids as a long chain acid were used. Two procedures for sample preparation were studied and their influence on the contact angle and corrosion resistance of the modified surface tested. The most effective pre-treatment procedure was optimized with respect to the type of carboxylic acid, its molarity and the immersion time. The electrochemical measurements were performed in a solution that simulates long-term outdoor exposure to urban rain.

2. EXPERIMENTAL

2.1 Materials

Samples were cut from 2 mm thick foil in the form of discs of 15 mm diameter. Copper (99.95 % purity) and zinc (99.5 % purity) were supplied by Goodfellow Cambridge Ltd and copper-zinc

alloys by Wieland-Werke AG, Ulm, Germany. The CuxZn alloys are denoted according to their zinc content: Cu10Zn and Cu40Zn, where x is zinc content in wt. %.

Myristic acid (MA) [tetradecanoic acid $C_{14}H_{28}O_2$, purity 98.5 %], decanoic acid (DA) [$C_{10}H_{20}O_2$, purity 98%] and hexanoic acid (HA) [$C_6H_{12}0_2$, purity 99.5 %], were supplied by Sigma-Aldrich Chemie GmbH, Germany. Stearic acid (SA) [octadecanoic acid, $C_{18}H_{36}O_2$, purity 97%] was supplied by ACROS-Organics. The acids were dissolved in absolute ethanol (Carlo Erba, Milan, Italy, purity 99.9 %) to concentrations of 0.01, 0.05 and 0.1 M.

Electrochemical measurements were performed in deionized water containing 0.2 g/L Na_2SO_4, 0.2 g/L $NaHCO_3$, 0.2 g/L $NaNO_3$ [27]. The pH was adjusted with 10% H_2SO_4 to pH 5 to simulate the acid rain present in polluted urban environments.

2.2 Preparation of samples

Metal samples were ground using, successively, 1200, 2400 and 4000-grid SiC emery papers, cleaned ultrasonically in ethanol for 5 minutes, rinsed with deionized water and dried in a stream of N_2. Further treatment of the samples involved two procedures. In the first, following grinding they were immersed in a solution of carboxylic acid in 0.05 M ethanol in water. In the second procedure the grinding was followed by etching in 10% HNO_3 for 30 s before immersion in the same ethanol-water solution of carboxylic acid. The samples were then dried in a stream of N_2 and electrochemical measurements carried out in simulated urban rain.

The following parameters were varied: the type of carboxylic acid (HA, DA, MA or SA), the time of immersion (1 min, 20 min, 1 day or 6 days) and the concentration of the carboxylic acid (0.01 M, 0.05 M and 0.1 M).

2.3 Electrochemical measurements

Electrochemical measurements were performed in simulated urban rain in a 1L corrosion cell K0047 (PAR) at room temperature. The working electrode was embedded in a Teflon holder with an exposed area of 0.95 cm^2. A graphite electrode served as a counter electrode and a saturated calomel electrode (SCE) was the reference electrode (E = 0.214 V). Measurements were performed using a potentiostat/galvanostat Parstat 2263 controlled by PowerSuite software. After 1 h stabilization at open circuit potential, potentiodynamic measurements were made from 250 mV negative up to 0.8 V (down to - 0.8 V for Zn) at a scan rate of 1 mV/s. Electrochemical parameters were determined by Tafel analysis using PowerSuite software. Each measurement was repeated at least three times.

2.4 Measurements of contact angle, surface roughness and surface morphology

Contact angles (Θ) were determined using a tensiometer Krüss DSA 20 (Krüss GmbH, Hamburg, Germany). They were measured based on the image of the deionized water drop on the sample surface, using Drop-shape-analysis software which enables fitting of the water drop on the

surface and enabling precise determination of the value of the contact angle. Each value is the average of at least three measurements made at different locations on the same sample.

Surface roughness was measured using the confocal microscope ZEISS Axio CSM 700 (Carl Zeiss AG, Göttingen, Germany) and evaluated by Axio Zeiss CSM 700 3-D software. Roughness was measured using a Z image over an area of 8400 μm^2. The results are expressed as average surface roughness, R_a, as the average of the absolute value of the height Z(x,y) in the measurement length, l = 1 mm, of the roughness curve in x and y directions. Each surface roughness value is the average of at least three measurements made at different locations on the same sample [28].

The morphology of modified samples was characterized by field-emission scanning electron microscopy (FEG-SEM, Jeol, JSM-7600F).

3. RESULTS AND DISCUSSION

3.1 The effect of surface preparation

The effects of grinding and etching on the hydrophobicity and corrosion inhibition of Cu, Zn, Cu10Zn and Cu40Zn surfaces were investigated. The changes in morphology and contact angles induced by etching are presented in Fig. 1.

Table 1. Mean values of surface roughness (R_a) and contact angles (Θ) for ground and etched bare samples.

sample	R_a / nm		Θ / °	
	ground	etched	ground	etched
Cu	53	76	47	63
Cu10Zn	74	168	42	59
Cu40Zn	74	145	68	69
Zn	114	154	61	74

Surface preparation affected the surface roughness (Table 1), which increased up to 2.3 times for etched samples. The brasses exhibited the greatest difference between the roughness of the ground and etched samples. Greater roughness of the etched surfaces was accompanied by larger contact angles. In both cases the surface was hydrophilic (Θ ≤ 90 °). Potentiodynamic curves for the bare ground and etched Cu and Zn samples and for modified samples immersed for 20 min in 0.05 M ethanol solution of SA are shown in Fig. 2. Values of electrochemical parameters, corrosion potential, E_{corr} and corrosion current density, j_{corr}, are presented in Table 2.

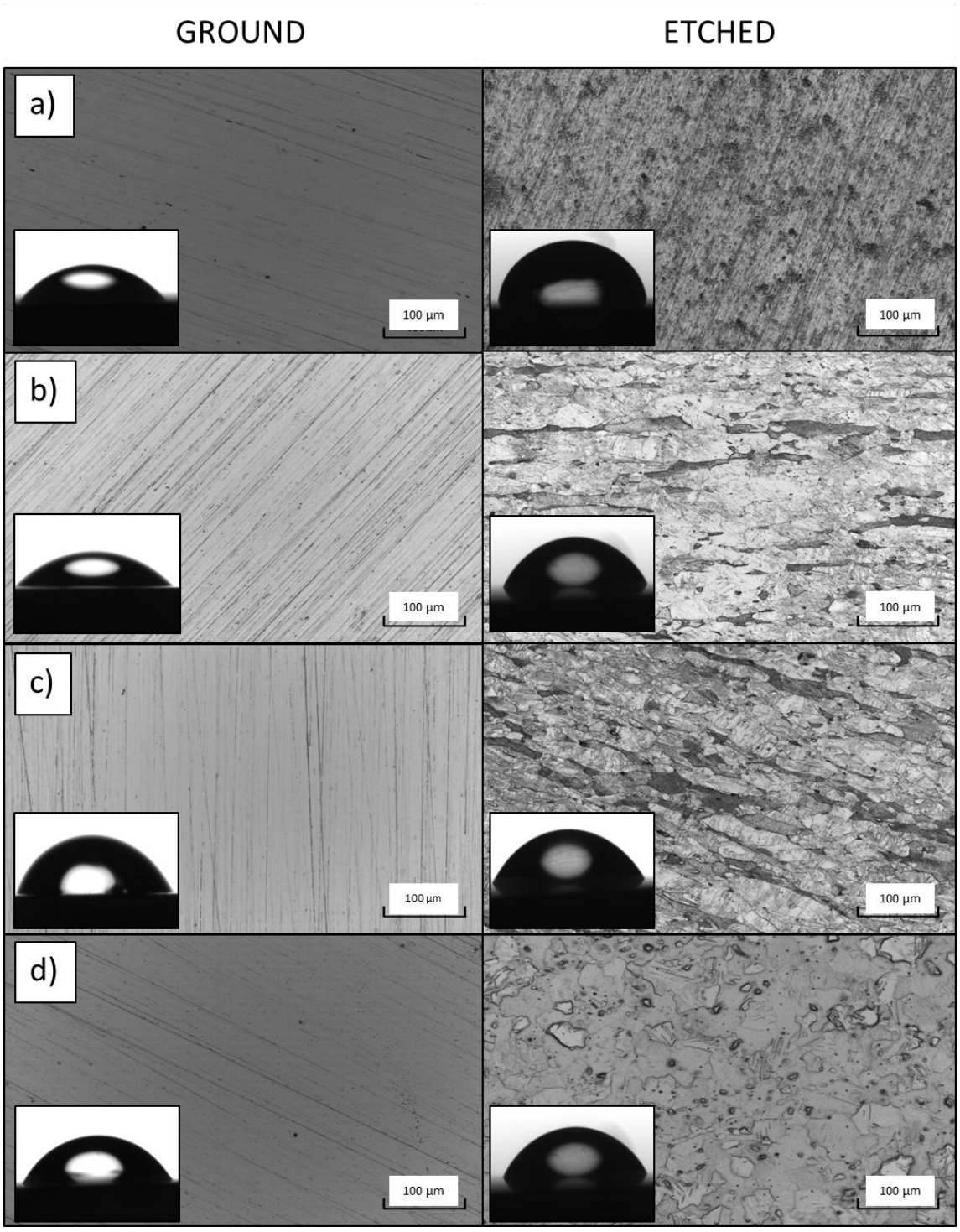

Figure 1. Images of ground and etched surfaces of Cu (a), Cu10Zn (b), Cu40Zn (c) and Zn (d) taken with a confocal microscope. Insets show the images of water drops. The resulting values of roughness and contact angles are presented in Table 1.

The results in simulated urban rain will be discussed first. No significant differences between bare ground and etched Cu samples (Table 2) were observed for Cu (Fig. 2a,b) and brasses.

Table 2. Electrochemical parameters, corrosion potential, E_{corr}, and corrosion current density, j_{corr}, for bare ground and etched samples. Samples were modified by immersion in 0.05 M stearic acid in ethanol for 20 min. Values of inhibition effectiveness (IE) are given.

sample	ground bare		etched bare		ground SA			etched SA		
	E_{corr} / mV	j_{corr} / μA cm^{-2}	E_{corr} / mV	j_{corr} / μA cm^{-2}	E_{corr} / mV	j_{corr} / μA cm^{-2}	IE / %	E_{corr} / mV	j_{corr} / μA cm^{-2}	IE / %
Cu	-53	3.130	-69	2.960	-47	0.125	96.0	-70	0.044	98.5
Cu10Zn	-66	3.040	-53	1.720	-53	0.123	95.9	-91	0.040	97.6
Cu40Zn	-91	3.850	-91	1.910	-69	0.047	98.7	-117	0.018	99.0
Zn	-1050	5.480	-1050	8.130	-987	5.370	1.8	-1030	4.140	49.1

The mechanism of Cu corrosion in simulated urban rain was not investigated in depth. The cathodic reaction in an acidic environment is reduction of oxygen which diffuses from the bulk solution and adsorbs on to the electrode surface [29]:

$$O_{2,bulk} \rightarrow O_{2,surf} \rightarrow O_{2,ads} \quad (3)$$

Mattson and Bockris [29] proposed that Cu dissolution in acidic sulphate system proceeds in two steps:

$$Cu \rightleftharpoons Cu(I)^{+} + e^{-} \text{ (fast) and} \quad (4)$$

$$Cu(I)^{+} \rightleftharpoons Cu(II)^{2+} + e^{-} \text{ (slow).} \quad (5)$$

At pH ≥ 3.5 the rate determining step is a film formation/dissolution process, while at pH ≤ 2.9 is a diffusion process of dissolved oxygen. Magaino suggested the formation of an intermediate Cu^{+}_{ads} [30]. This species associates with an anion X^{n-} to form a complex $(Cu^{+})_n X^{n-}$ which then diffuses into the bulk solution:

$$n\ Cu^{+}_{ads} + X^{n-}_{surf} \rightarrow [(Cu^{+})_n X^{n-}]_{surf} \rightarrow [(Cu^{+})_n X^{n-}]_{bulk} \quad (6)$$

Depending on the electrolyte composition, various types of solid corrosion products can be formed at the water-copper interface [31]. Simulated rain used in this work contains NO_3^-, HSO_4^-, SO_4^{2-} and other anions, and the formation of compounds such as Cu_2S, Cu_2O, CuS, $CuSO_4 \times 5\ H_2O$, etc., can be expected.

For Zn, the difference between ground and etched samples is larger; etched samples showed a more positive corrosion potential for ~ 200 mV and a plateau in the cathodic region (Figs. 2c,d). The shape of the etched curve is consistent with both $2e^-$ and $4e^-$ oxygen reduction coupled with ZnO reduction [32]. At potentials about 500 mV lower than E_{corr}, hydrogen generation occurs by reduction of water (eq. 7):

$$2H_2O + 2e^{-} \rightarrow H_2 + 2OH^{-} \quad (7)$$

and the ZnO film formed during sample preparation is reduced to Zn. As the potential becomes more positive the rate of H_2 evolution decreases. On oxide-free zinc the current density stabilizes with the $4e^-$ oxygen reduction process taking place:

$$O_2 + 2H_2O + 4e^{-} \rightarrow 4OH^{-} \quad (8)$$

At more positive potentials, Zn oxidation to ZnO begins. As the surface starts to be covered with ZnO the rate of $4e^-$ oxygen reduction decreases and that of the $2e^-$ process increases:

$$O_2 + 2H_2O + 2e^- \rightarrow HO_2^- + OH^- \quad (9)$$

$$HO_2^- + H_2O + 2e^- \rightarrow 3OH^- \quad (10)$$

Further polarization results in the electrode becoming covered with ZnO and oxygen reduction via the $2e^-$ reaction stops. At potentials more positive than E_{corr} dissolution of zinc begins (eq. 11).

$$Zn \rightarrow Zn^{2+} + 2e^- \quad (11)$$

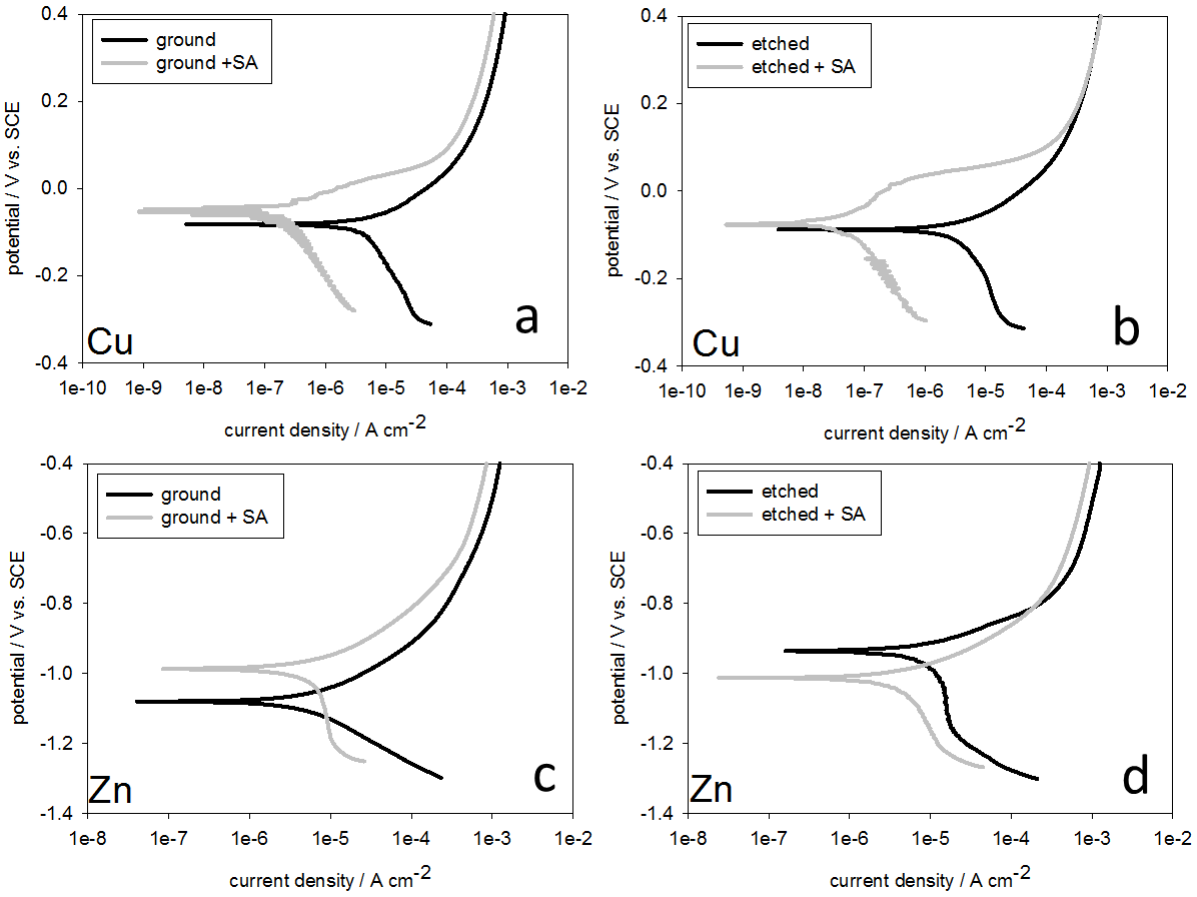

Figure 2. Polarization curves for bare ground (a, b) and etched (c, d) samples of Cu and Zn recorded in simulated urban rain. Samples were modified by 20 min immersion in a 0.05 M ethanol solution of stearic acid (SA).

Magaino et. al. [33] suggested that the initial step of zinc dissolution in simulated acid rain is the charge transfer reaction resulting in formation of adsorbed species, Zn^+_{ads}. It is not clear whether Zn^+_{ads} is oxidised to Zn^{2+} ions directly or through the formation of Zn^{2+}_{ads}. In aerated Na_2SO_4 solution Zn^I, Zn^{II} and $ZnOH_{ads}$ species have been proposed [34].

Potentiodynamic curves recorded for ground and etched Cu and Zn samples modified by SA are presented in Fig. 2. The results for brasses are given in Table 2. The effect of SA was larger on Cu than on Zn. For Cu, both cathodic and anodic current densities were reduced. For the etched sample the decrease was up to two orders of magnitude, while for Zn the effect was greater for the cathodic part.

The inhibition effectiveness, IE, of the modified surfaces was calculated according to the equation (12):

$$IE(\%) = \frac{j_{corr(bare)} - j_{corr(mod)}}{j_{corr(bare)}} * 100 \quad (12)$$

where $j_{corr(bare)}$ and $j_{corr(mod)}$ are the corrosion current densities for a bare surface and for a surface modified by carboxylic acid. SA achieved IE values ranging from 49% for Zn to 99% for Cu40Zn (Table 2). The values for Cu and brasses were similar and ranged from 96% to 98.5 %. Etched samples showed higher IE values than ground samples. The difference in IE between ground and etched sample was the highest for Zn (~ 40%), while that for Cu and alloys was up to 5%.

Contact angles of samples immersed in SA were generally higher for etched than for ground samples (Table 3). Compared to unmodified samples (Table 1), samples modified in SA exhibited a hydrophobic surface ($\Theta \geq 90°$). Based on these results, further measurements were performed on etched samples since they were more inhibition effective.

Table 3. Mean values of contact angles (Θ) of water drops measured on etched surfaces of samples after immersion in 0.05 M stearic acid in ethanol for 20 min.

sample	Θ / °	
	SA, ground	SA, etched
Cu	110	114
Cu10Zn	94	101
Cu40Zn	104	104
Zn	105	122

3.2 The effect of carboxylic acid chain length

Potentiodynamic curves for bare and modified samples recorded in simulated urban rain are presented in Fig. 3. Regardless of the length of carboxylic acid, both anodic and cathodic reactions on Cu were suppressed (Fig. 3a). The decrease in current density increased with increasing length of the carbon chain. For Cu samples modified in DA, MA and SA, a passive region was observed. The IE increased from 34% for HA to 98.5% for SA (Fig. 4). For both brasses modified with HA (Fig. 3b and 3c) the cathodic and anodic current density was greater than that for bare samples and, consequently, the IE is negative (Fig. 4). For brasses modified with DA, MA and SA, the current density was less with increasing carbon chain length. Consequently, the inhibition effectiveness, IE, was greater. The formation of a passive range was not so pronounced for brasses as for Cu, except for Cu10Zn in MA solution. The carboxylic acids act as a mixed type of inhibitor for Cu and brasses because they influence the cathodic and anodic current density.

Self-assembled layers of n-alkanoic acid ($CH_3(CH_2)_mCOOH$), m=2-18,22) were easily formed on the native oxide surfaces of Cu [15]. The Cu^+ ions react with n-alkanoic acid molecule to form copper carboxylate:

$$Cu^+ + CH_3(CH_2)_mCOOH \rightarrow Cu[CH_3(CH_2)_mCOO] + H^+ \quad (13)$$

In the case of released Zn^{2+} ions, zinc carboxylate can form according to the following reaction [35]:

$$Zn^{2+} + 2CH_3(CH_2)_mCOOH \rightarrow Zn[CH_3(CH_2)_mCOO]_2 + 2H^+ \quad (14)$$

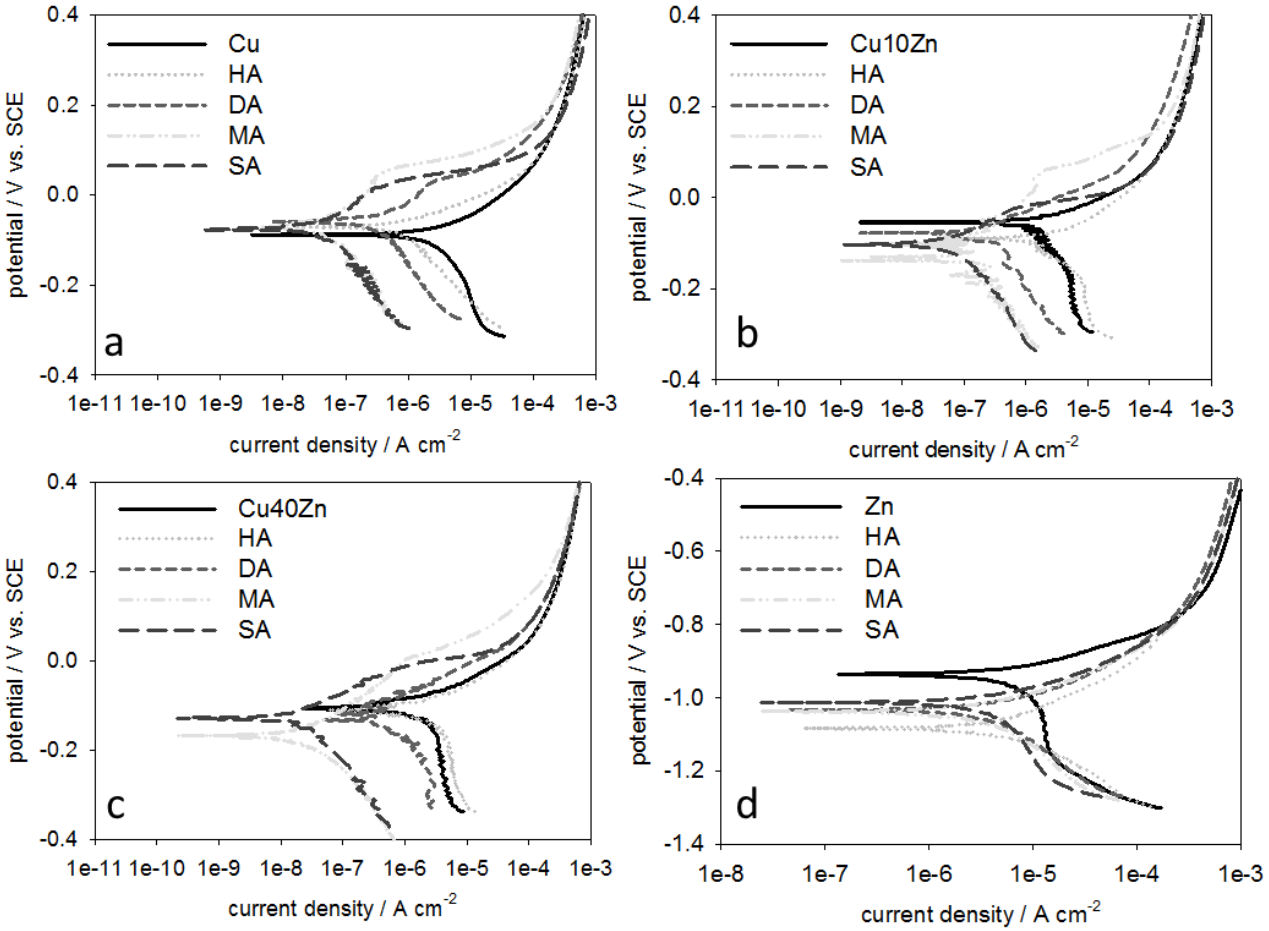

Figure 3. Polarization curves for etched bare and modified Cu (a), Cu10Zn (b), Cu40Zn (c) and Zn (d) in artificial simulated urban rain. Modified surfaces were prepared by 20 min immersion of the samples in 0.05 M ethanol solution of hexanoic acid (HA), decanoic acid (DA), myristic acid (MA) and stearic acid (SA).

The IE of modified Zn samples increased with increasing carbon chain length from 23 % for HA to 49 % for SA (Fig. 4). For Zn, carboxylic acids act mainly as cathodic inhibitors. As for Cu and brasses, the largest difference was observed between HA and DA, while MA and SA showed similar IE values.

The contact angles of modified samples were more than 90° for all acids (Table 4). Values of contact angles did not increase linearly with increasing length of the carbon chain. In the case of Cu and Zn they were highest in SA, for Cu10Zn in HA and, for Cu40Zn, the contact angle was highest in DA. The difference of contact angles in various acids was not statistically significant. Boisier et al. [10] reported that the contact angles for surfaces modified with different carboxylic acids do not change after the carbon chain length of the carboxylic acid was long enough to confer a hydrophobic

effect. In the present work the length of the carbon chain was observed to affect the inhibition effectiveness to a greater extent than it affects the values of contact angles (Table 4, Fig. 4).

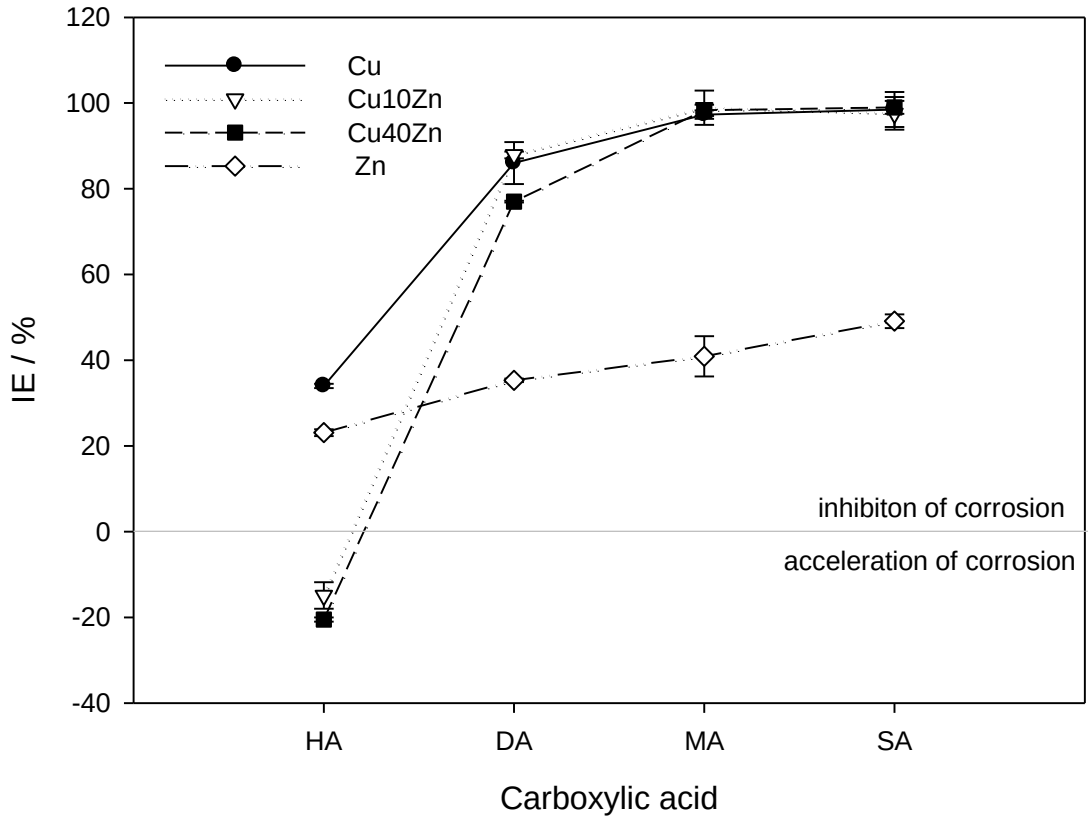

Figure 4. The effect of length of carboxylic chain of the carboxylic acid (hexanoic acid (HA), decanoic acid (DA), myristic acid (MA) and stearic acid (SA)) on the inhibition effectiveness (IE) for Cu, Zn, Cu10Zn and Cu40Zn immersed for 20 min.

Table 4. Mean values of contact angles (Θ) of water drops measured on surfaces of etched bare samples and etched samples after 20 min immersion in 0.05 M ethanol solution of different carboxylic acids (hexanoic acid (HA), decanoic acid (DA), myristic acid (MA) and stearic acid (SA)).

sample	**Θ / °**				
	bare, etched	HA	DA	MA	SA
Cu	63	104	111	96	114
Cu10Zn	59	108	104	92	101
Cu40Zn	61	98	106	100	104
Zn	74	100	113	104	122

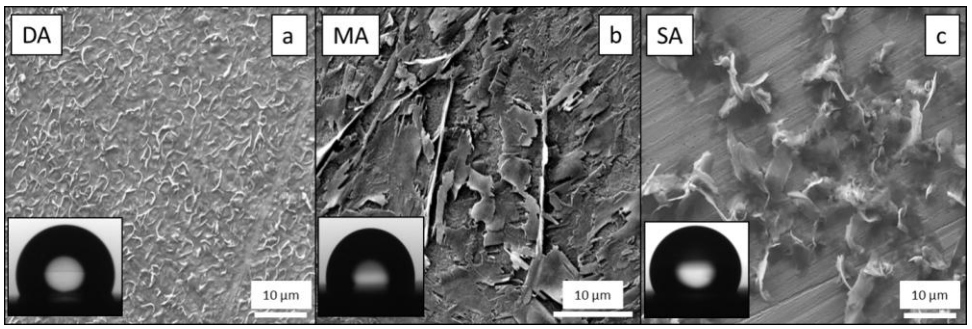

Figure 5. SEM images of an etched Cu surface after 20 min immersion in 0.05 ethanol solution of a) decanoic acid (DA), b) myristic acid (MA) and c) stearic acid (SA). Insets show the images of water drops; the resulting contact angles are presented in Table 5.

SEM images of the surface of self-assembled layers formed on Cu after 20 min immersion in 0.05 M ethanol solution of DA (Fig. 5a), MA (Fig. 5b) and SA (Fig. 5c) are presented. DA formed a self-assembled layer which completely covered the surface of Cu (Fig. 5a). The layer was thinner than in the case of MA and SA. The MA formed a self-assembled layer of plates of different size and shape (Fig. 5b). The SA formed flower-like clusters; the surface underneath can be observed indicating that it was not completely covered (Fig. 5c). These results lead to the conclusion that carbon chain length of the carboxylic acid affects the morphology of the self-assembled layers. For the samples presented in Fig. 5 the values of contact angle ranged from 111° for HA to 96° for MA and 114° for SA (Table 4).

3.3 The effect of immersion time

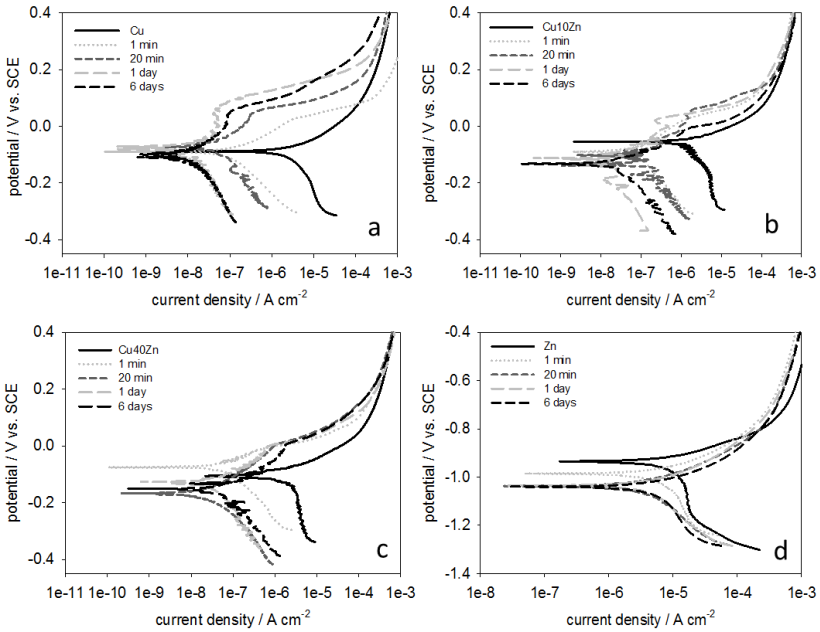

Figure 6. Polarization curves for etched bare and modified Cu (a), Cu10Zn (b), C40Zn (c) and Zn (d) in simulated urban rain. The surfaces were modified by immersion of the samples in 0.05 M ethanol solution of myristic acid (MA) for different times of immersion (1 min, 20 min, 1 day and 6 days).

The effect of immersion time on the effectiveness of inhibition and the hydrophobicity was investigated for Cu, Zn, Cu10Zn and Cu40Zn immersed in 0.05 M ethanol solutions of MA and SA, for immersion times from 1 min to 6 days. Potentiodynamic curves of the modified samples were measured in simulated urban rain (Fig. 6 for MA and Fig. 7 for SA). The IE values are presented in Fig. 8.

3.3.1 Myristic acid

Modified surfaces of Cu in a 0.05 M ethanol solution of MA showed, compared to bare Cu, cathodic and anodic current densities lower by up to two orders of magnitude after 1 min and 20 min immersion, and by up to three orders of magnitude after immersion for 1 day and 6 days (Fig. 6a). A passive region was established whose extent increased with increasing time of immersion. The corrosion potentials of modified Cu samples did not change significantly compared to those for bare Cu. IE for Cu was already high after 1 min immersion and reached a maximum value of 99.4% for a 1 day immersion, and then remained similar for up to 6 days (Fig. 8a).

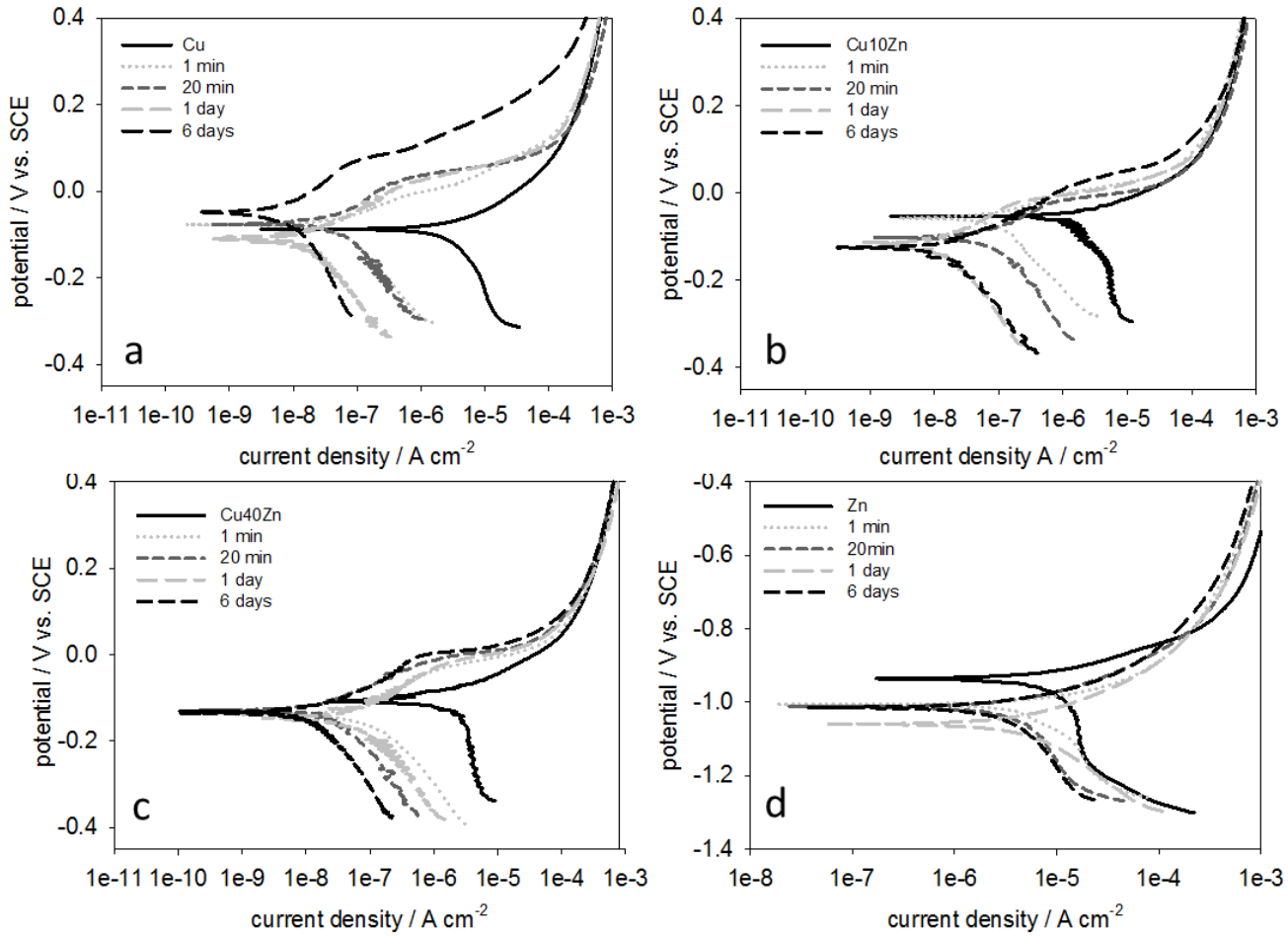

Figure 7. Polarization curves for etched bare and modified Cu (a), Cu10Zn (b), Cu40Zn (c) and Zn (d) in simulated urban rain. The surfaces were modified by immersion of the samples in 0.05 M ethanol solution of stearic acid (SA) for different times (1 min, 20 min, 1 day and 6 days).

Corrosion potentials for modified Cu10Zn samples were shifted negatively relative to the bare sample (Fig. 6b). The cathodic and anodic current densities decreased by up to two orders of magnitude after 6 days immersion. As for copper, a passive region was established for the modified samples. The IE was 95.0 % after 1 min immersion, increased to 99.8 % for a 1 day immersion and slightly less after a 6 days immersion (Fig. 8a). Modified samples of Cu40Zn behaved similarly to Cu10Zn samples (Fig. 6c). The IE increased, reaching a maximum after 20 min immersion, and then decreased to 96.5 % for 6 days immersion (Fig. 8a).

Modified samples of Zn showed a lower cathodic current density, and a shift of corrosion potential in the negative direction relative to bare samples (Fig. 6d). No passive region was observed. Much lower IE values were obtained than for Cu and brasses. IE increased from 22 % for 1 min immersion to 41 % for 20 min immersion and then remained relatively constant for up to 6 days (Fig. 8b).

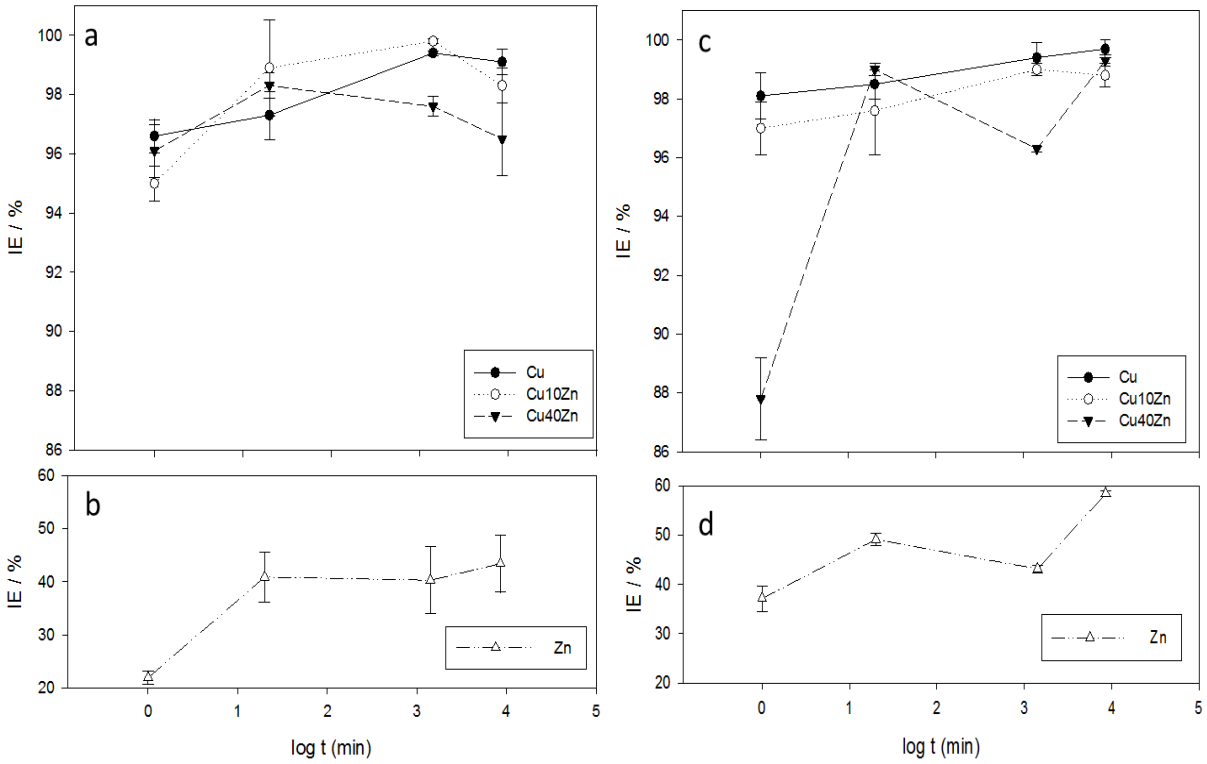

Figure 8. The effect of immersion time on inhibition effectiveness (IE) for Cu, Zn, Cu10Zn and Cu40Zn immersed in 0.05 M ethanol solution of myristic acid (a,b) and stearic acid (c,d). Mean values with standard deviations are presented.

3.3.2 Stearic acid

Potentiodynamic curves of Cu samples modified in ethanol solutions of SA (Fig. 7a) for different immersion times and recorded in simulated urban rain were similar to those for MA (Fig. 6a). The passive region was established after 1 min immersion and its extent increased with longer immersion. The corrosion potentials for 1 min, 20 min and 6 day's immersion shifted slightly in the

positive direction relative to the bare sample; only for 1 day's immersion was it shifted in the negative direction. The IE increased with increasing time of immersion from 98.1 % after 1 min to 99.7 % after 6 days (Fig. 8c). The dependence of IE on immersion time was similar to that for samples immersed in MA. The IE for samples immersed in SA was slightly higher than those for MA.

The current densities for modified Cu10Zn and Cu40Zn (Figs. 7b and 7c) samples decreased by two orders of magnitude with increasing immersion time. The shape of the curve was similar to that for MA, as well as for the values of IE (Fig. 8c). For Cu40Zn the value of IE was quite low (~88 %) after 1 min immersion, but increased with longer immersion (Fig. 8c). Cu40Zn samples immersed in MA for 1 min and 1 day had a higher IE than when immersed in SA. The cathodic and anodic current densities of modified Zn samples decreased, but a further increase in immersion time did not significantly affect the current density (Fig. 7d). Compared to MA, the IE values were higher.

SEM images of self-assembled layers (Fig. 9) were taken after various immersion times (20 min, 1 day and 6 days) for Cu (Fig. 9a, 9b and 9c) and Zn (Fig. 9d, 9e and 9f) in 0.05 M ethanol solutions of SA. After 20 min immersion there were some flower-like clusters about 10 μm in diameter on the surface of Cu (Fig. 9a). The surface was not completely covered with these clusters as the bare Cu surface could be seen underneath.

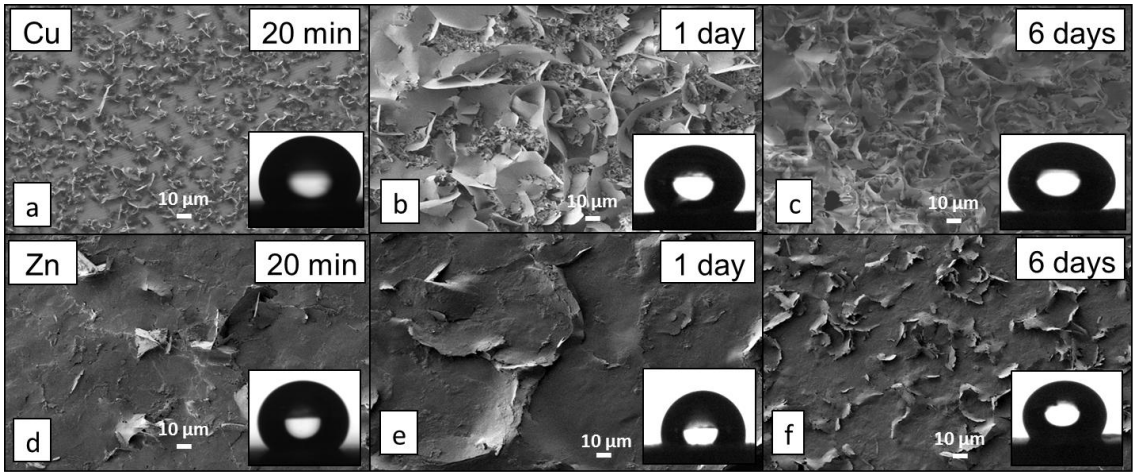

Figure 9. SEM images of Cu (a, b, c) and Zn (d, e, f) surfaces after immersion in 0.05 ethanol solution of stearic acid (SA) for different times of immersion (20 min, 1 day and 6 days). Inserts show the images of water drops; the resulting contact angles are presented in Table 5.

The contact angle of the surface was 114° and the IE 98.5 % (Table 5). After 1 day of immersion the clusters grew in size and density and the surface was completely covered with small and larger flower-like sheets (Fig. 9b). Nano-particles were formed between the sheets. These sheets allow air to be trapped more easily in the small caves on the surface. The contact angle and the IE increased (136° and 99.4 %) compared to 20 min immersion (Table 5). After 6 days immersion the surface of Cu was fully covered with sheets that were more similar in size and shape to each other (Fig. 9c). The contact angle and IE were almost the same as after 20 min immersion (135° and 99.7 %) (Table 5). Flower like structures formed in the presence of SA on surface of Cu have been observed by other authors [14,36].

Table 5. Mean values of contact angles (Θ) and inhibition effectiveness (IE) for Cu and Zn after immersion for 20 min, 1 day and 6 days in 0.05 M ethanol solutions of stearic acid.

sample	time of immersion					
	20 min		1 day		6 days	
	Θ / °	IE / %	Θ / °	IE / %	Θ / °	IE / %
Cu	114	98.5	136	99.4	135	99.7
Zn	122	49.1	106	43.1	128	58.4

Clusters of plates were formed on Zn after 20 min immersion in ethanol solution of SA (Fig. 9d). Individual plates grew with increasing immersion time. After 20 min immersion, the contact angle decreased from 122° to 106° after 1 day immersion. At the same time the IE decreased from 49.1 % to 43.1 % (Table 5). After 6 days immersion the surface of Zn was covered with clusters of plates (Fig. 9f) but to a much smaller extent than the surface of Cu (Fig. 9c). The contact angle and IE increased to 128° and 58.4 %. There is a clear relationship between the changes in surface morphology and the resulting parameters: dense plate-like structures on Cu showed higher contact angle and IE than the modified Zn surface.

These results confirm that the same carboxylic acid can form different shapes of self-assembled layers on different metals [17]. The time of immersion affected the density and the size of clusters formed on the surface. The process of self-assembly of the layers was rapid, since samples modified after 1 min immersion in MA exhibited IE above 90 % for Cu and brasses, but only 21 % for Zn. For SA, the IE were over 87 % for Cu and brasses, and much less (37.1 %) for Zn (Fig. 8).

3.4 The effect of concentration

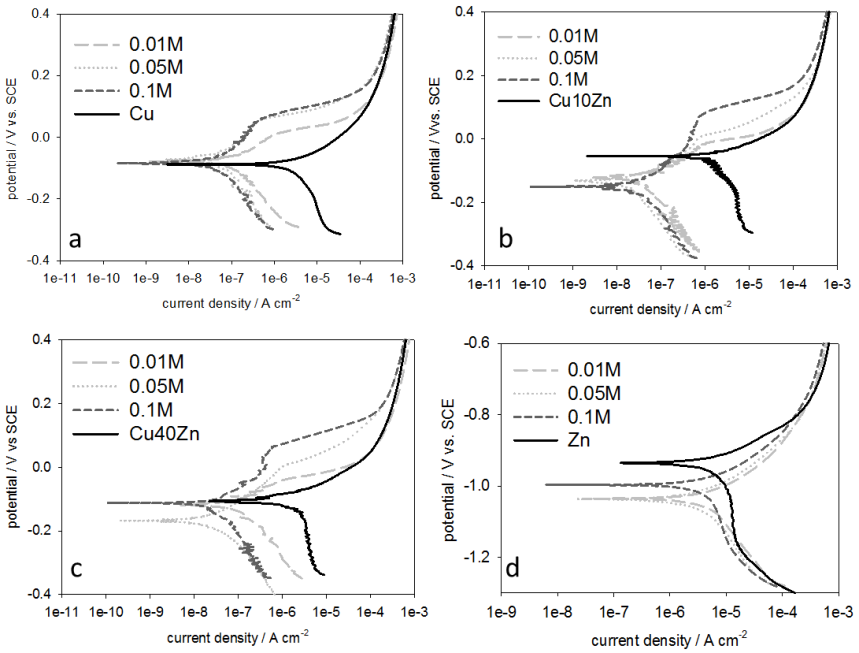

Figure 10. Polarization curves for etched bare and modified Cu (a), Cu10Zn (b), Cu40Zn (c) and Zn (d) in simulated urban rain. The surfaces were modified by 20 min immersion of the samples in 0.01 M, 0.05 M and 0.1 M ethanol solution of myristic acid (MA).

The effect of molarity of MA and SA (from 0.01 M to 0.1 M) on the effectiveness of inhibition and on contact angles was investigated following 20 min immersion. Potentiodynamic curves in simulated urban rain for the modified samples are presented in Fig. 10 for MA and Fig. 11 for SA. The corrosion parameters are presented in Fig. 12a and 12b for MA and, for SA, in Figs. 12c and 12d.

3.4.1 Myristic acid

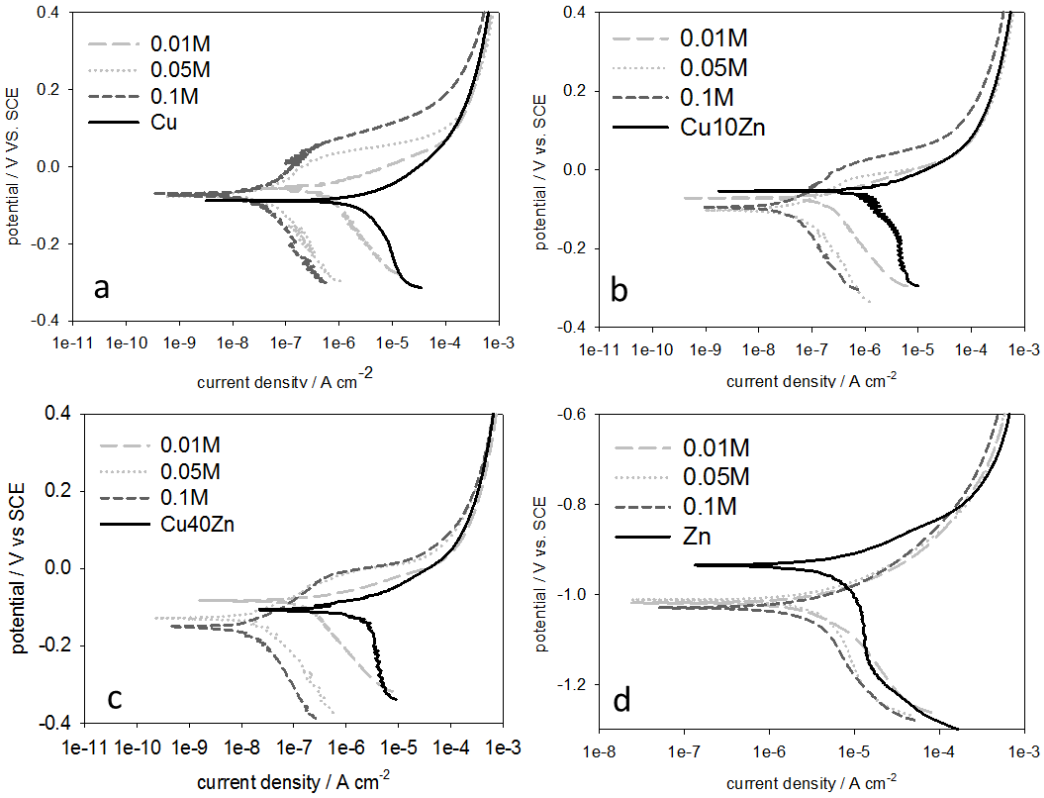

Figure 11. Polarization curves for etched bare and modified Cu (a), Cu10Zn (b), Cu40Zn (c) and Zn (d) in simulated urban rain. The surfaces were modified by 20 min immersion of the samples in 0.01 M, 0.05 M and 0.1 M ethanol solution of stearic acid (SA).

Values of corrosion potentials for modified Cu (Fig. 10a) samples had values similar to those for bare Cu. For the modified samples, the anodic and cathodic current densities decreased by up to three orders of magnitude and a passive region was established which increased with increasing molarity. The IE was high (96 - 97 %) for all concentrations tested (Fig. 12a). The contact angle decreased from 114° to 97° with increasing molarity (Table 6). For modified Cu10Zn and Cu40Zn (Fig. 10b and 10c), the values of E_{corr} were shifted more in the negative direction than for Cu. The shape of the curve was similar to that for Cu, the extent of the passive region depending on the molarity of the acid. Both alloys reached high IE values, similar to those for Cu (Fig. 12a), and also similar contact angles (Table 6).

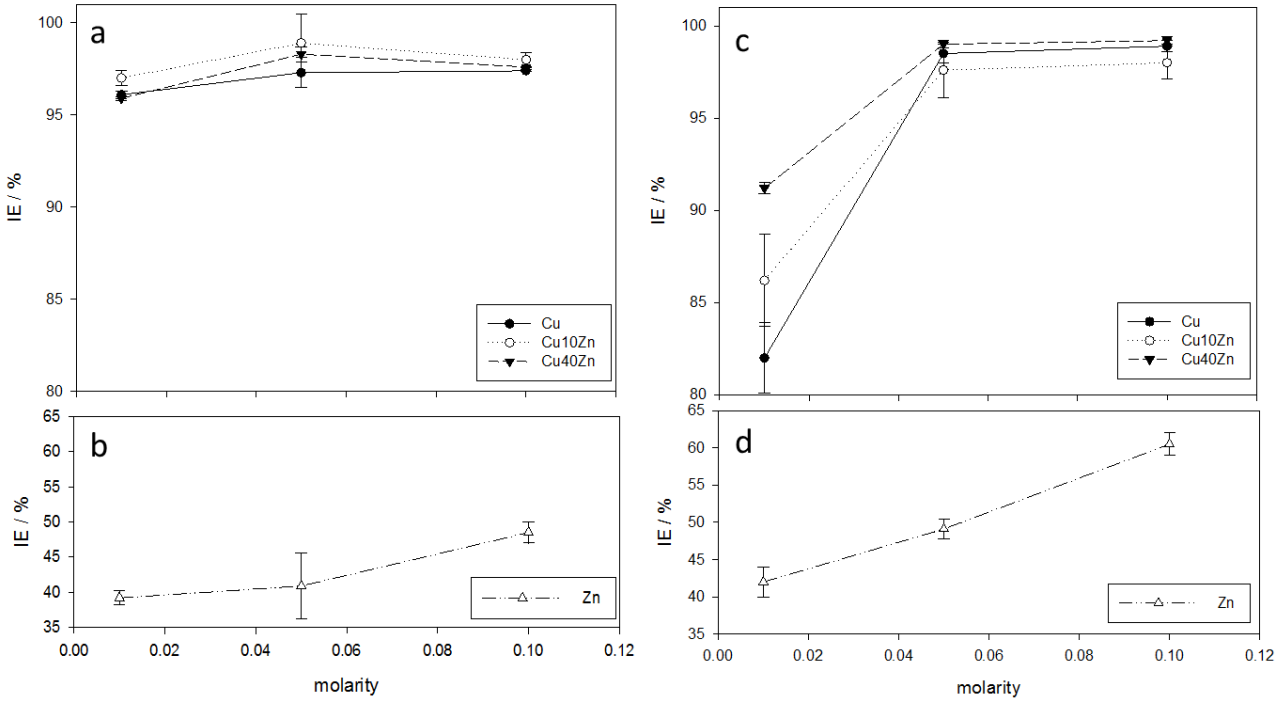

Figure 12. The effect of the molarity of myristic acid (MA) (a,b) and stearic acid (SA) (c,d) in ethanol solution on the inhibition effectiveness (IE) for Cu, Zn, Cu10Zn and Cu40Zn immersed for 20 min. Mean values and standard deviations are presented.

Table 6. Mean values of contact angles (Θ) of water drops measured on surfaces of etched samples modified by immersion for 20 min in solutions containing various molar concentrations of myristic (MA) and stearic acid (SA) in ethanol.

sample	Θ / °					
	MA			SA		
	0.01 M	0.05 M	0.1 M	0.01 M	0.05 M	0.1 M
Cu	114	96	97	109	114	106
Cu10Zn	100	92	92	103	101	100
Cu40Zn	103	100	104	104	104	104
Zn	103	104	97	103	122	101

Corrosion potentials of modified Zn (Fig. 10d) samples were shifted in the negative direction compared to those for bare Zn. The IE increased from 39.2 % to 48.5 % with increasing molarity (Fig. 12b). The contact angles for 0.01 M and 0.05 M were almost the same and decreased slightly for a 0.1 M solution (Table 6).

3.4.2 Stearic acid

Except for a slight positive shift of E_{corr}, the shape of the curve for Cu in SA was as that for MA (Fig. 11a). However, the IE achieved at low molarity was much lower than for MA, but was greater in more concentrated solutions (Fig. 12a). The IE was 82 % for 0.01 M and 98.9 % for 0.05 M

solution (Fig. 12c). The contact angle increased from 109° for 0.01 M to 114° and then decreased to 106° (Table 6). As observed for Cu, the passive region of modified Cu10Zn and Cu40Zn samples increased with increasing molarity (Fig. 11b and 11c). At the same time the values of current density decreased over the whole potential range. The corrosion potentials were shifted in the negative direction. The contact angles were almost the same for all molarities (Table 6). Both alloys reached similar IE values (Fig 12c). Polarization curves for Zn are similar to those in MA (Fig. 10d). The values of contact angle were between 103° and 122° (Table 6). The IE increased from 42 % for 0.01 M to 60.5 % for 0.1 M solution (Fig. 12d).

Summarizing the results of the effect of acid molarity (Fig. 12), the largest difference was observed at low molarity (0.01 M). For Cu and brasses the values of IE were high (> 95 %) in MA but substantially lower in SA. For concentrations ≥ 0.05 M, high IE were achieved in both acids. For Zn, the IE values were higher in the presence of SA. The contact angles did not increase with increasing molarity of the carboxylic acids, indicating that the self-assembled layers are already hydrophobic at low molarity.

4. CONCLUSIONS

The effect of carboxylic acids as corrosion inhibitors for Cu, Zn and brasses, tested in simulated urban rain, is dependent on the pre-treatment, type of metal, type of carboxylic acid, the concentration of the latter and the period of immersion.

-Using the etching procedure as a pre-treatment, higher surface roughness, larger contact angles and better corrosion resistance were achieved compared to the ground sample. Pre-treatment was essential for achieving high inhibition effectiveness.

-Carboxylic acids achieved high IE (95 %) on Cu and Cu10Zn, somewhat less on Cu40Zn, and relatively little (~ 50 %) on Zn.

-The IE increased with increasing carbon chain length of the carboxylic acids. MA and SA are better corrosion inhibitors than the short chain acids HA and DA. For brasses, HA even acts as a corrosion accelerator. MA achieved better inhibition at a lower concentration (0.01 M) than SA, which peaked at 0.05 M and then levelled-off slightly at 0.1 M. In contrast, the effect of SA increased at 0.05 M and remained stable at 0.1 M.

-All carboxylic acids formed a hydrophobic, self-assembled layer. Contact angles were more than 90°. The morphology of layers differed for different carboxylic acids, longer chains allowing air to be trapped in the holes and groves. The contact angles were independent of the length of the carbon chain. The results show that carboxylic acids with different carbon chain lengths form different shapes of self-assembled layers on same metal, and the same carboxylic acid forms differently shaped self-assembled layers on different metals.

-The time of immersion in ethanol solution affects the inhibition effectiveness of carboxylic acids. Self-assembly is a rapid process, an IE of over 87 % being achieved after just 1 min immersion for Cu and brasses, and over 21 % for Zn.

-Zn was affected by immersion time more than Cu and alloys, which achieved much higher values of IE at all immersion times tested. Plate-like morphology, including nanoparticles, was formed on Cu in stearic acid, with the number of plates increasing with increasing immersion time. This micro textured surface provided an effective barrier to corrosive solutions. Furthermore, the surfaces became hydrophobic. The layers formed on Zn show a much smaller number of plate-like products, indicating that the morphology affects the effectiveness of inhibition.

-The optimum conditions for corrosion protection of Cu, Zn and brasses include the etching of the surface of bare samples for 30 s in 10 % HNO_3, the use of long carbon chain carboxylic acids and longer immersion times (in days).

ACKNOWLEDGEMENTS
The Slovene Research agency is acknowledged for financial support (grant no. P2-0148). The authors thank Prof. Dr. Barbara Malič for contact angle measurements and Peter Rodič for technical assistance.

References

1. 1. M. Finšgar, I. Milošev, *Corros. Sci.*, 52 (2010) 2737.
2. M. M. Antonijević, M.B. Petrović, *Int. J. Electrochem. Sc.*, 3 (2008) 1.
3. P. Qui, D. Persson, C. Leygraf, *J. Electrochem. Soc.*, 156 (2009) C441.
4. T. Kosec, D. Kek Merl, I. Milošev, *Corros. Sci.*, 50 (2008) 1987.
5. S. Thomas, N. Birbilis, M.S. Venkatraman, I.S. Cole, *Corrosion*, 68 (2012) 015009-1.
6. T. Liu, L. Dong, T. Liu and Y. Yin, *Electrochim. Acta*, 55 (2010) 5281.
7. Q. Wang, B. Zhang, M. Qu, J. Zhang and D. He, *Appl. Surf. Sci.*, 254 (2008) 2009.
8. Y. Yin, T. Liu, S. Chen, T. Liu and S. Cheng, *Appl. Surf. Sci.*, 255 (2008) 2978.
9. S. Ren, S. Yang, Y. Zhao, T. Yu, X. Xiao, *Surf. Sci.*, 546 (2003) 64.
10. G. Boisier, A. Lamure, N. Pebere, N. Portail and M. Villatte, *Surf. Coat. Tech.*, 203 (2009) 3420.
11. Z. Chen, L. Hao, A. Chen, Q. Song and C. Chen, *Electrochim. Acta*, 59 (2012) 59.
12. P. Wang, R. Qui, D. Zhang, Z. Lin and B. Hou, *Electrochim. Acta*, 56 (2010) 517.
13. L. Xu, L.M. Dong and W. Li, *Colloid. Surface. A*, 404 (2010) 12.
14. S.-W.Chen, B.L. Guo and W.-S. Wu, *Appl Phys A*, 105 (2011) 861.
15. T. Liu, S. Chen, S. Cheng, J. Tian, X. Chang and Y. Yin, *Electrochim. Acta*, 52, (2007) 8003.
16. S. Wang, L. Feng and L. Jiang, *Adv. Mater.*, 18, (2006) 767.
17. I. Milošev, T. Kosec and M. Bele, *J. Appl. Electrochem.*, 40 (2010) 1317.
18. W.F. Ng, M.H. Wong and F.T. Cheng, *Surf. Coat. Tech.*, 204 (2010) 1823.
19. Y. Wan, Z. Wang, Y. Liu, C. Qi and J. Zhang, *Tribol. Lett.*, 44 (2011) 327.
20. H. Liu, S. Szunertis, W. Xu and R, Boukherroub, *ACS Appl. Mater. Inter.*, 1 (2009) 1150.
21. P.V. Mahalakshmi, S.C. Vanithakumari, J. Gopal, U. Kamachi Mudali and B. Raj, *Curr. Sci. India*, 101 (2011) 1328.
22. T. Liu, Y. Ying, S. Chen, X. Chang and S. Cheng, *Electrochim. Acta*, 52 (2007) 3709.
23. S. Zheng and J. Li, *J. Sol-Gel Sci. Technol.*, 54 (2010) 174.
24. W. Xu, H. Liu, S. Lu, J. Xi and Y. Wang, *Langmuir*, 24 (2008) 10895.
25. P. Wang, D. Zhang, R. Qiu and B. Hou, *Corros. Sci.*, 53 (2011) 2080.
26. A. Marmur, *Langmuir*, 19 (2003) 8343.
27. T. Kosec, A. Legat and I. Milošev, *Prog. Org. Coat.*, 69 (2010) 199.
28. I. Milošev and B. Kapun, *Mater. Sci. Eng. C*, 32 (2012) 1087.
29. E. Mattson and J. O`M Bockris, *Trans. Faraday. Soc.*, 55 (1959) 1586.
30. S. Magaino, *Electrochim. Acta*, 42 (1997) 377.

31. R. Winston Revie, *Uhlig`s Corrosion Handbook (2nd edition)*, John Wiley & Sons, New York (2000).
32. H. J. Flitt, D. P. Schweinsberg, *Corros. Sci.*, 52 (2010) 1905.
33. S. Magaino, M. Soga, K. Sobue, A. Kawaguchi, N. Ishida and H. Imai, *Electrochim. Acta*, 44 (1999) 4307.
34. C. Deslouis, M. Duprat, Chr. Turnillon, *Corros. Sci.*, 29 (1989) 13.
35. P. Wang, D. Zhang, R. Qiu and B. Hou, *Corros. Sci.*, 53 (2011) 2080.
36. Y. Wang, W. Wang, L. Zhong, J. Wang q. Jiang and X. Guo, *Appl. Surf. Sci.*, 256 (2010) 3837.